Trees (2021) 35:527–541
https://doi.org/10.1007/s00468-020-02054-y

ORIGINAL ARTICLE

A quantitative evaluation of soil mass held by tree roots

Toko Tanikawa[1,2] · Hidetoshi Ikeno[3] · Chikage Todo[4,7] · Keitaro Yamase[4] · Mizue Ohashi[3] · Toru Okamoto[2] · Takeo Mizoguchi[2] · Katsuhiro Nakao[2] · Shinji Kaneko[2] · Atsushi Torii[2] · Yoshiyuki Inagaki[5] · Asami Nakanishi[6] · Yasuhiro Hirano[7]

Received: 16 July 2020 / Accepted: 17 October 2020 / Published online: 16 November 2020

Abstract

Key message **Tree roots hold soil that is dramatically heavier than the tree biomass, wet or dried. This soil might compensate for the imbalance between above- and belowground mass.**

Abstract Root–soil plates are recognized to play an important role in root anchorage of plate-like root system, however, actual measurements of their mass have rarely been reported. Even though the root–soil plate mass is often estimated using aboveground allometric indices, no research confirms the validity. Seven root–soil plates of *Cryptomeria japonica* fallen by Typhoon Jebi were divided into roots and soil, and their weights were directly measured. Mass of the seven plates ranged from 251 to 3070 kg on a dry basis. Roots accounted for 8% of total plate mass and soil for 92%. The mass of the soil held in the plates was 2.8 times greater than tree biomass. The root-to-shoot biomass ratio was 0.26, whereas the ratio of root–soil plate mass to shoot biomass was 3.9, meaning that the root–soil plate mass was much greater than aboveground biomass. These results suggest that the soil mass held in the plate is the main component of whole-tree mass including the plate. The root system holds soil weighing as much as 13 times the root system's mass. The soil might balance the aboveground weight of the tree by adding mass. Aboveground allometric indices are good indicators of root–soil plate mass and allow the belowground mass to be estimated to understand tree anchorage without soil disturbance.

Keywords Disaster · Root anchorage · Root–soil plate · Tree stability · Uprooting · Windthrow

Introduction

Root anchorage is an important factor in a tree's tolerance of slope failures associated with intense rainfall and storms, which are becoming more frequent with climate change, and against tsunamis associated with huge earthquakes. Windthrow studies in forests have gained popularity over the last few decades because of the importance of tree stability to both the environment and society (Sagi et al. 2019). Some recent studies have focused on the stability of coastal trees against tsunami disasters (e.g., Nanko et al. 2019; Todo et al. 2019). Tree-pulling experiments and simulations of tree uprooting processes, such as the finite element method, have been adopted to improve our understanding of tree anchorage (Dupuy et al. 2005a, b, 2007; Fourcaud

Communicated by DesRochers .

Electronic supplementary material The online version of this article (https://doi.org/10.1007/s00468-020-02054-y) contains supplementary material, which is available to authorized users.

✉ Toko Tanikawa
toko105@agr.nagoya-u.ac.jp

1 Graduate School of Bioagricultural Sciences, Nagoya University, Nagoya 464-8601, Japan

2 Kansai Research Center, Forestry and Forest Products Research Institute, 68 Nagaikyutaro, Momoyama, Fushimi, Kyoto 612-0855, Japan

3 School of Human Science and Environment, University of Hyogo, Himeji, Hyogo 670-0092, Japan

4 Hyogo Prefectural Technology Center for Agriculture, Forestry and Fisheries, Shiso, Hyogo 671-2515, Japan

5 Shikoku Research Center, Forestry and Forest Products Research Institute, 2-915 Asakuranishi, Kochi 780-8077, Japan

6 Field Science Education and Research Center, Kyoto University, Kyoto 603-8047, Japan

7 Graduate School of Environmental Studies, Nagoya University, Nagoya 464-8601, Japan

et al. 2008; Yang et al. 2018). Key factors determining root anchorage are root architecture (Danjon et al. 2005; Dupuy et al. 2005a, b, 2007; Yang et al. 2018), soil shear strength (Dupuy et al. 2005a; Nicoll et al. 2006; Yang et al. 2018), root–soil plate (RSP) properties, such as shape and mass (Coutts 1986), and the location of the rotation axis of uprooting (Dupuy et al. 2005a, 2007). Recording local responses of the root–soil system has identified the windward and leeward roots, soil strength, and RSP mass as the main components of anchorage (Coutts 1983, 1986; Dupuy et al. 2005a, b, 2007; Fourcaud et al. 2008; Ghani et al. 2009; Stokes 1999; Yang et al. 2017).

The contribution of each factor to root anchorage seems to vary among root system architectures and tree age. Lateral windward roots provide the greatest resistance to overturning for many trees (e.g. Coutts 1983; Crook et al. 1997) and allow adaptation to wind load because of their highly branched pattern of growth (Stokes et al. 1995). The importance of the taproot for root anchorage depends on tree age. Previous studies showed that the taproot is the main component of root anchorage, but that its importance is decreased in mature trees (Crook and Ennos 1998; Dorval et al. 2016; Toral et al. 2011). On the other hand, only trees with tap root or heart root systems receive the benefits of soil shear strength (Mattheck et al. 2015). Trees with plate-like root systems or buttress roots are like trees planted in containers due to their own mass and RSP mass (Mattheck et al. 2015). For trees planted in containers, the fracture moment of the trunk is proportional to the soil mass (Mattheck et al. 2015). In a Sitka spruce (*Picea sitchensis*), which has a shallow root system, the second-most important anchoring factor after lateral windward roots is RSP mass (Coutts 1983, 1986). The RSP represents the association between the root system and its adhering soils (Coutts 1986). RSPs are usually observed in tree-pulling experiments, in which stem size and mass, RSP dimensions (Cucchi et al. 2004; Nicoll et al. 2006), and root system architecture (Khuder et al. 2007) are measured. Despite the importance of RSP mass, only one study has measured it directly (Coutts 1986). Some reasons for the lack of data might be that direct measurement requires time and labor, and cases where RSP mass plays an important role in root anchorage are limited. Although RSP mass has been estimated from aboveground allometric indices, such as stem diameter at breast height (DBH), no research has confirmed the validity of RSP mass estimation from aboveground allometric indices. Nanko et al. (2019) stated that direct measurements of RSP properties are needed to increase the accuracy of numerical simulation of tree stability.

Root biomass is usually smaller than aboveground biomass. For firm anchorage of trees with plate-like root systems, it is crucial that their small root systems hold a large amount of soil. Understanding the balance between aboveground biomass and RSP mass or between root biomass and soil mass in the RSP might be useful to evaluate the soil-holding efficiency of a root system. The relative weight balance of a tree, between above- and belowground biomass, is commonly expressed as the root-to-shoot ratio, indicating biomass allocation (Klepper 1991). Ennos (1993) noted that although root-to-shoot ratios are usually analyzed from a biological perspective, they can be modified to indicate tree stability. This ratio varies with mean annual precipitation, mean annual temperature, forest stand height, stand/tree age (Mokany et al. 2006), and soil type or soil nutrients (Vogt et al. 1995). Cairns et al. (1997) performed a global meta-analysis of root-to-shoot ratios for upland forests and reported variation ranging from 0.05 to 0.7. Mokany et al. (2006) also analyzed root-to-shoot ratios in global terrestrial biomes and showed that the average value in forest ecosystems is 0.26. These values indicate that the weight balance is too biased toward the aboveground portions to expect tree stability, based on tree biomass alone. One component that may compensate for this imbalance is soil held by roots, that is, within the RSP. We defined the RSP as a mechanism for increasing the belowground weight of an individual tree. Our first hypothesis is that RSP mass is equal to or greater than the mass of the aboveground part of the tree.

Not only the mass but the shape properties of the RSP are important parameters for anchorage estimation. Achim and Nicoll (2009) focused on the resistance offered by windward roots and RSP mass as the most important components of anchorage, and they showed that root anchorage can be modelled as proportional to the square of RSP spread. Fourcaud et al. (2008) also reported that, in their simulation, the shape and size of RSP alter anchorage, even when some elements of the root system are removed. The model showed that all elements of the root system contribute to anchorage in purely sandy soils, whereas only the longest element has a large contribution in clay soil. Thus, it is important that soil type and root architecture be used in combination to evaluate root anchorage. The radius and thickness of an RSP also depend on its root system architecture. If soil environments limiting tap root development interfere with the exhibition of species-specific root architecture, this may alter the radius and/or thickness of an RSP. In soil with high penetration resistance or with a shallow ground water table, tap roots might not develop, causing all RSPs to become flat regardless of species-specific differences in root architecture. Our second hypothesis is that the sizes of RSP, RSP radius and thickness, are the same for all trees growing in hard soil when standardized by tree size, regardless of species-specific root architecture.

Trees felled by typhoons or windstorms offer an opportunity to gather information on the mass and dimensions of RSPs. An intense, very large typhoon, the local name for a tropical cyclone in the western Pacific, can leave huge RSPs

on the ground. Typhoon Jebi, which formed on 28 August 2018, struck Japan on 4 September 2018 as a Category 3 typhoon on the Saffir–Simpson scale (i.e., 1-min maximum sustained winds of 50–58 m s^{-1}; Takabatake et al. 2018). The typhoon uprooted many trees in the Kinki district and left complete RSPs on the ground. During Typhoon Jebi, instruments in Kyoto city measured an instantaneous wind speed of 39.4 m s^{-1}, the maximum value recorded since the end of World War II (Kyoto Local Meteorological office). Coutts (1986) calculated that 13 m s^{-1} is required for uprooting a *Picea sitchensis* tree with DBH of 15.3 cm, and a slightly higher speed (14–17 m s^{-1}) is required for trees with DBH of 18.5–26.7 cm. Although whether the trunk snaps or the tree is overturned is mediated not only by wind speed, but also by RSP properties including previous partial failures, the maximum wind speed of Typhoon Jebi was so high that the wind uprooted or broke many trees in this region.

To improve our understanding of root anchorage, the objectives of this study were (i) to quantitatively evaluate the soil mass held by the root system of *C. japonica*, and (ii) to confirm whether the RSPs of different tree species growing in hard soil are similar in shape. We also aimed to confirm whether aboveground allometric indices reflect RSP mass. We divided RSPs of *Cryptomeria japonica* with various DBH values growing in hard soil in a forest damaged by Typhoon Jebi into soil and root portions and directly measured their mass. The intrinsic root type of *Cryptomeria japonica* is deep rooting depth and a heart root system (Table 1). We also measured radius and thickness of RSPs in multiple species of trees with various types of root systems. We sampled trees species classified as deep-, intermediate-, and shallow-rooted types by Karizumi (2010), based on exhaustive digging surveys of mature tree root systems in Japan. Heart, tap, and plate-like root architectures as defined by Köstler et al. (1968) and similarly defined by Karizumi (2010) (Table 1). In tree-pulling experiments, trees are commonly pulled from one direction without shaking. Yang et al. (2020) indicated that the successive wind gusts may damage trees, lowering their critical overturning bending moment compared to that predicted by tree-pulling experiments. Furthermore, trees are generally crushed more in natural uprooting than in pulling experiments. For these reasons, the RSPs sampled here may have been smaller than those in previous tree-pulling experiments.

Materials and methods

Study site

Typhoon Jebi traversed the Kinki district of Japan on 4 September 2018, causing devastating damage to forests. In the damaged area, covering 1595 ha of 11 prefectures across Japan, the economic value of damaged forest trees amounted to about 4 million US dollars (Ministry of Agriculture, Forestry and Fisheries 2019).

We conducted an RSP survey across about 1 ha of a mixed forest of conifers and broad-leaved trees at the Kansai Research Center, Forestry and Forest Products Research Institute (FFPRI site, 34°56′N, 135°46′E, 70 m altitude), Kyoto, Kinki district, Japan. The dominant tree is *C. japonica*, which is planted frequently and covers 44% of the plantation forest area in Japan (Forest Agency of Japan 2012). Mean annual air temperature in 2018 was 16.9 °C and annual precipitation was 1770 mm at the nearest weather station (Kyoto station, AMeDAS, Japan Meteorological Agency). The soil was classified as Inceptisols (Soil Survey Staff

Table 1 Categorization of sample trees according to Köstler et al. (1968) and Karizumi (2010)

Tree species	According to Karizumi (2010)				According to Köstler et al. (1968) [d]	Number of samples	
	Rooting depth[a]	Lateral root type[b]	Branches[c]	Fine roots[c]		RSP mass and volume	RSP shape
Cryptomeria japonica	Deep	Intermediate	Intermediate	Many	Heart root system	7[e]	13
Quercus acutissima	Deep	Convergent	Intermediate	Sparse	Tap-root system	0	1
Quercus myrsinifolia	Intermediate	Convergent	Many	Sparse	Heart root system	0	8 (7)[f]
Quercus glauca	Intermediate	Convergent	Many	Sparse	Heart root system	0	2
Zanthoxylum ailanthoides	Intermediate	Intermediate	Sparse	Sparse	Heart root system	0	1
Chamaecyparis obtusa	Shallow	Convergent	Many	Many	Plate-like root system	0	5 (4)[f]

[a]Deep, intermediate, or shallow

[b]Dispersion, intermediate, or convergent

[c]Many, intermediate, or sparse

[d]Heart, taproot, or plate-like. Karizumi (2010) also classified root systems using similar terms

[e]Sample IDs were C1–C7

[f]Number in parentheses is for RSP thickness. Thickness was not measured for two trees with RSPs with collapsed bottoms

2014), and the texture was clay loam. Slope gradient class was flat according to FAO guidelines (Jahn et al. 2006).

The forest was devastated by Typhoon Jebi and many trees were uprooted by the strong winds, falling on other trees and toppling them as well. Because neighboring trees fell one after another, almost all trees on the site were uprooted, perhaps not only trees with poor root anchorage. The crowns of the fallen trees often overlapped, and numerous RSPs were broken by other falling trees. We collected weather data for the day that Jebi landed from the Kyoto station of AMeDAS (Japan Meteorological Agency). To test the first hypothesis, we chose seven (C1–C7) uprooted *C. japonica* trees (Table 2). The number of samples was limited because we only selected fully exposed RSPs that had retained their original shapes with little or no collapse. Most of the other uprooted RSPs were damaged by surrounding fallen trees and had been cleaned up immediately after the storm to restore the forest. Thus, we took the rare opportunity to collect data on these seven RSPs immediately after the storm event. We measured the mass, radius, and thickness of RSPs, as well as the aboveground allometric indices and fall directions of the trees. The stand density was not uniform in the site: 728 trees ha^{-1} around C1 and C2, 113 trees ha^{-1} around C3 and C4, and 2916 trees ha^{-1} around C5, C6, and C7. Details of the mass, radius, and thickness measurements are described below. The fall directions of the sample trees were measured using a compass glass. To test the second hypothesis, radius and thickness of the uprooted RSPs and DBH were measured for 30 trees: the seven *C. japonica* plus an additional six, eight *Quercus myrsinifolia*, two *Q. glauca*, one *Q. tacutissima,* one *Zanthoxylum ailanthoides*, and five *Chamaecyparis obtusa*. Root architecture types classified according to the categories of Köstler et al. (1968) and by the Japanese conventional root categories of Karizumi (2010) are shown in Table 1.

Root–soil plate mass of *Cryptomeria japonica*

The seven uprooted RSPs were divided into roots and soil and their masses were directly measured. Before measuring the mass of an uprooted RSP, radius, thickness, and hinge ratio of the plate and aboveground allometric indices of the sample trees were assessed as described below, and the stem was cut off at about 50 cm aboveground. Tree age was estimated by counting the tree rings of a cross section of the cut stem at ground level (0 cm) after division of the uprooted RSPs.

We first removed roots extending out from the uprooted RSPs and the mass of these roots (outside roots) was determined directly using a hanging scale. Then, the living roots in soils at the hinge side (Fig. 1) were also cut off. Because we did not measure the fresh weight of the outside roots for C5, we calculated it based on the dry biomass and the

Table 2 Properties of sample trees and their root–soil plates of *Cryptomeria japonica*

Tree ID	DBH	Height	Tree age	Root–soil[a] plate mass	Soil mass	Total root biomass[a]	V_{full}[b]	$V_{uprooted}$[b]	Aboveground biomass	Tree biomass[a]	Nearest soil trench profile
	(cm)	(m)	(year)	(kg dw)	(kg dw)	(kg dw)	(m^3)	(m^3)	(kg dw)	(kg dw)	
C1	31	21	43	675	636	39	0.99	0.67	353	392	Profile 1
C2	44	21	43	3070	2880	192	4.45	3.03	705	897	Profile 2
C3	19	16	33	451	419	32	0.60	0.38	111	143	Profile 3
C4	25	17	33	678	618	61	1.13	0.95	224	285	Profile 4
C5	23	15	26	817	778	39	1.36	0.88	117	156	Profile 5
C6	22	17	27	646	551	95	1.40	0.91	125	220	Profile 5
C7	16	14	26	251	221	29	0.68	0.50	60	89	Profile 6
Mean ± SD	25 ± 9	17 ± 3	33 ± 3	941 ± 957	871 ± 902	70 ± 59	1.52 ± 1.33	1.05 ± 0.90	242 ± 226	312 ± 277	

[a]This value does not include roots on the tipped-up side of the RSP that were torn off during uprooting

[b]V_{full} indicates the volume of the RSP including the hinge side, whereas $V_{uprooted}$ indicates RSP volume excluding the hinge side

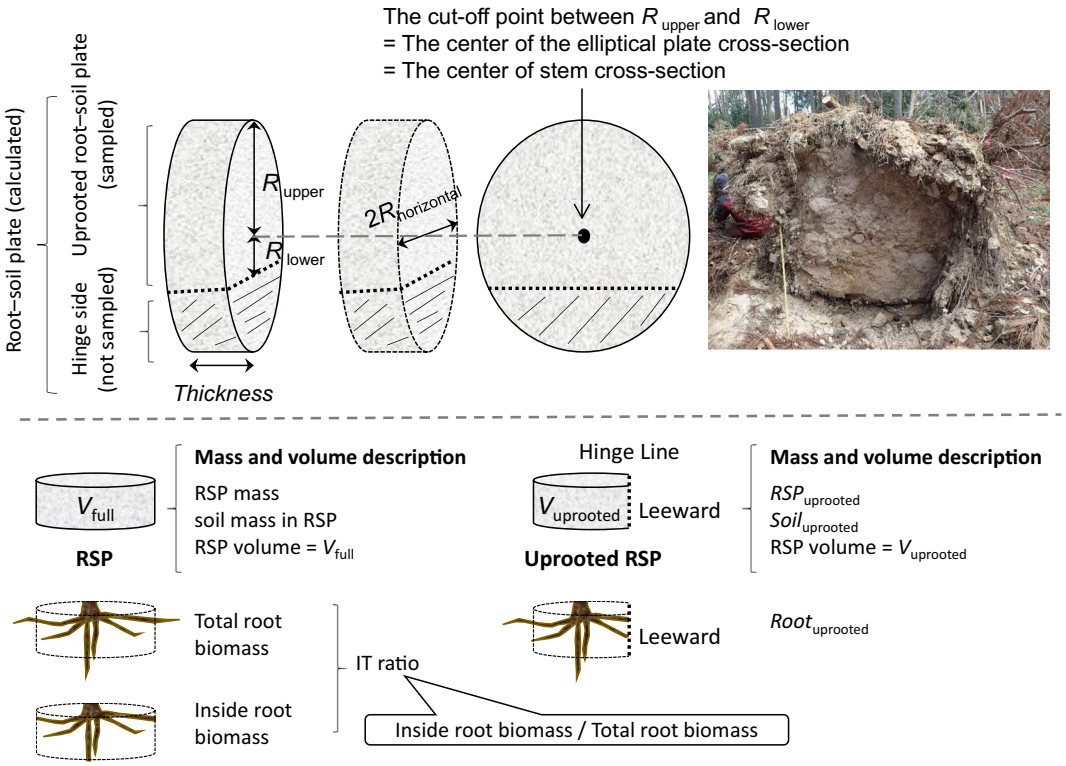

Fig. 1 Measured parts of a root–soil plate. $2R_{horizontal}$ (horizontal diameter), thickness, R_{upper} (vertical radius of the upper side) and R_{lower} (vertical radius of the lower side) are shown. The ratio of V_{full} to $V_{uprooted}$ was used to reconstruct the mass of the hinge side of root–soil plates by Eqs. (2), (3), and (4)

root water contents of subsamples from the six other sample trees. The root biomass of uprooted RSPs ($Root_{uprooted}$) included outside roots of the uprooted RSPs. However, it included neither living roots in soils at the hinge side nor roots on the tipped-up side torn off by uprooting. The uprooted RSP mass ($RSP_{uprooted}$) and its soil ($Soil_{uprooted}$) did not include hinge side. We hung whole RSP or a fragment of a plate either on the arm of an excavator (ViO30, Yanmar Co., Ltd., Osaka, Japan) with wire rope or a belt sling or on a tripod with a chain block and wire rope. A load cell (maximum load 50 kN, LT-50KNG56 Nikkei Electronic Instruments Co. Ltd, Tokyo, Japan) was connected between the belt sling and wire rope, and the mass was recorded using a strain unit (EDX-11A, Kyowa Electronic Instruments Co., Ltd., Tokyo, Japan) (Fig. S1 of Supplementary materials). After removal of the load cell from the hanging system, the soil was removed from the hanging RSP using crowbars, pickaxes, hammers, shovels, chisels, and screwdrivers. The falling soil was intercepted by plastic sheets and/or plastic containers, and the mass of each batch of removed soil was measured using a balance scale. If $RSP_{uprooted}$ exceeded the load capacity of the excavator or the chain block to lift, we divided the uprooted RSP into several pieces on a plastic sheet. The mass of the trunk cut at 0 cm aboveground was also measured and excluded from $RSP_{uprooted}$. Fresh masses of both $Root_{uprooted}$ and soil ($Soil_{uprooted}$) were immediately measured using the load cell or the balance scale in the field. In the case of C2, the plate was too heavy and too large to lift on the arm of the excavator, so we made a trench around the plate and dropped soil from the plate onto plastic sheets or containers in the trench using shovels and other tools (Fig. S2 of Supplementary materials). The soil that was firmly adhered to the stump was removed with the bucket of the excavator by rocking or tapping gently. The fallen roots and soil were collected separately. After initial soil removal, the uprooted RSPs were cut into smaller pieces using a chain saw, and the pieces were separated into soil and roots on plastic sheets spread on the ground. As for the other plates, the stump of C2 was separated into the aboveground (stem) and belowground parts (roots), and the fresh masses of the roots and soil were measured. Subsamples of soil and roots were oven-dried at 105 °C and 80 °C, respectively, for 10 days to determine their water contents. Wood tissue density was also calculated from the root subsamples. All values are reported on an oven-dry mass basis.

Radius, thickness, and hinge ratio of the root–soil plates

The radius and thickness of the uprooted RSPs were measured manually for a total of 30 trees, including the seven *C. japonica* (C1–C7). Lundström et al. (2007a) reported that the shape of an RSP is described well by a depth-dependent taper model with an elliptical cross section. However, perhaps due to a hard and shallow soil horizon, the roots were not developed sufficiently downward to show a taper in this study. Figure 1 shows an example that is representative of all seven trees. Thus, we measured the both of radius and thickness of the RSP as an elliptical-based cylinder having the horizontal diameter in the direction parallel to the ground ($2R_{\mathrm{horizontal}}$) (Fig. 1). Two stainless steel rulers were placed on each side of an RSP—the ground surface side and the bottom—and the distance between the rulers was taken as the thickness of the plate. Since the bottom of each RSP was uneven, the thickness was measured four times on each plate, and the average value was used. For the seven *C. japonica*, the vertical radii of the upper side (R_{upper}) and the lower side (R_{lower}) were also measured. Hinge ratio is defined as the ratio of R_{lower} to R_{upper}. This ratio was used for calculation of the volumes of the uprooted RSPs.

Soil properties

Six soil profiles were made from trenches 70 cm wide and 80–90 cm deep. The bottom of each profile was so hard that we could not make it deeper. Soil samples were collected from three depth categories (0–10 cm, 35–45 cm, 50–80 cm) from each profile. In the profiles, we measured soil penetration resistance using the soil hardness tester designed by Yamanaka (Ref. No. 351, Fujiwara Scientific Co., Tokyo, Japan) for the uppermost horizon (0–10 cm deep), the second horizon (35–45 cm deep), and the deepest horizon (50–80 cm deep). Penetration resistance was calculated as follows:

$$\text{penetration resistance}\left(\text{kg cm}^{-2}\right) = (100X)/0.7952(40-X)^2, \quad (1)$$

where X is the Yamanaka soil hardness index (reading, mm) (Yamanaka and Matsuo 1962). Then 100-cm^3 soil cores were collected from the three depth categories from each profile. A three-phase soil meter (DIK-1150, Daiki, Tokyo, Japan) was used to measure the proportions of solid, liquid, and gas in the soil core samples. On the day Typhoon Jebi struck the forest, the volumetric soil water content at 0–6 cm depth was 20.2 ± 0.9% (mean ± SD), as measured every 30 min for 24 h using a soil moisture monitor equipped with 60-mm rods (ThetaProbeML2x, Delta-T Devices Ltd., Cambridge, UK) (Takanashi et al., unpublished data). This value was measured with four rods that had been buried in the ground at points 15 m away from the nearest RSP (C5).

Calculation and statistical analysis

To estimate the volumes of the RSPs, we first calculated the volume of an elliptical-based cylinder with radius ($R_{\mathrm{horizontal}}$ and R_{upper}) and height (thickness of the plate), as V_{full} (Fig. 1). Then, the part leeward of the hinge was subtracted from the volume of the elliptical-based cylinder in R statistical software, version 3.5.3 using the hinge ratio (R Development Core Team 2019), as V_{uprooted}. The mass was corrected using the following equations to restore the part to the leeward of the hinge:

$$\text{RSP mass} = \text{RSP}_{\mathrm{uprooted}} \times V_{\mathrm{full}}/V_{\mathrm{uprooted}}, \quad (2)$$

$$\text{Soil mass of RSP} = \text{Soil}_{\mathrm{uprooted}} \times V_{\mathrm{full}}/V_{\mathrm{uprooted}}, \quad (3)$$

$$\text{Total root biomass} = \text{Root}_{\mathrm{uprooted}}(\text{inside roots}) \times V_{\mathrm{full}}/V_{\mathrm{uprooted}} + \text{Root}_{\mathrm{uprooted}}(\text{outside roots}). \quad (4)$$

We defined the IT ratio as the ratio of the biomass of inside roots to that of total roots. Tree biomass was calculated as the sum of aboveground and total root biomass. Aboveground biomass was calculated as the sum of leaf, branch, and stem biomasses. According to Inagaki et al. (2020), leaf and branch biomasses can be estimated by the following method which is based on the pipe model theory (Shinozaki et al. 1964). Equations adopted in the method to estimate the biomasses using height (H, m), height at the lowest living branch (HB, m) and stem cross-sectional area at 1.3 m height ($A_{1.3}$, m^2) were follows:

$$\text{Leaf biomass (kg)} = a \times A_{1.3} \times (H-\text{HB})/(H-1.3)/1000, \quad (5)$$

$$\text{Branch biomass (kg)} = b \times A_{1.3} \times (H-\text{HB})/(H-1.3)/1000, \quad (6)$$

where a and b are the coefficients for a tree species, $A_{1.3}$ was calculated from the measurement of diameter at breast height (DBH). The coefficients (a and b) were estimated from two felled trees in the study site (24.5 cm and 24.8 cm in DBH). Since the coefficient of the pipe model is not affected by tree size, sampling of two trees would be enough for this estimation. In each tree, HB, $A_{1.3}$ and basal area of all branches were measured. Three branches were taken from the upper, middle and lower parts of the crown. Leaf and branch biomass of the whole tree is estimated by multiplying

basal area of all branches by the mean value of biomass per unit of branch basal area of the two felled trees. The mean value of coefficient (a and b) of the two trees was 1295 kg m^{-2} and 728.85 kg m^{-2} for leaf and branch, respectively. Stem volume was estimated by an open-source stem volume calculation program (Forestry and Forest Product Research Institute 2010) using measured values of DBH and *H* as independent variables. The program was established by Hosoda et al. (2010). Stem biomass (kg) on a dry basis was calculated from the stem volume and the wood tissue density. Aboveground allometric parameters, DBH, *H*, HB, and tree age, were measured directly in the field survey, except for HB of C5, C6, and C7. Before we could measure the HB values, the aboveground parts of C5, C6, and C7 were quickly cleared away as part of typhoon recovery. Instead of direct measurement, HB and *H* were measured for 10 trees surrounding C5, C6, and C7, and then a linear equation of HB with *H* was obtained. Using the equation, HB of C5, C6, and C7 was estimated from *H*.

The root-to-shoot ratio was calculated as the ratio of total root biomass to aboveground biomass. We also calculated the ratio of RSP mass to aboveground biomass, reflecting the weight balance, to help us understand tree stability.

We used both power and linear regression analyses to determine the relationships of aboveground allometric indices to mass or volume of uprooted RSPs and their components ($RSP_{uprooted}$, $Soil_{uprooted}$, $Root_{uprooted}$, $V_{uprooted}$). In this analysis, we used both fresh and dried weights of RSP components, because during the storm, the important components were the fresh weight of the tree, which determined the load on the root system; the wet weight of the soil; and the fresh weight of the roots. The aboveground allometric indices comprised DBH, stem biomass, aboveground biomass, $H \times DBH^2$, and stem taper index (height/DBH ratio). The analysis was conducted first for all samples (the seven *C. japonica* trees), and second for all samples excluding C1 (the RSP of a rotted tree) and C2 (the largest RSP). Linear regression analyses were performed between DBH and $R_{horizontal}$ or thickness for all 30 RSPs. The same analysis was performed to determine the relationship between $RSP_{uprooted}$ and $V_{uprooted}$. These analyses were performed with the SPSS software package (version 23; IBM, Chicago, IL, USA) and the IGOR Pro software (version 6.03; WaveMetrics, Inc., Portland, OR, USA).

Results

Change in the direction of strong wind

According to recordings at the Kyoto station of AMeDAS (Japan Meteorological Agency), the strong swirling wind of the typhoon had attacked trees from mainly two directions within a short time (Fig. S3b of Supplementary materials). At 14:30, the wind direction suddenly changed, and at the same time, the maximum instantaneous wind speed of the date was recorded. Perhaps the eye of Jebi passed over our study site at this moment. We define the wind at the time from 00:00 to 14:30 as the first attack, and the wind from 14:30 to 24:00 as the second attack. Six of the seven sample trees (except C3) fell in directions ranging from north to east, and this direction matched the wind direction of the second attack (Fig. S3a of Supplementary materials). What caused the sample trees' fatal damage and led them to uproot was probably the second attack after the eye of Jebi had passed. Although the first attack probably felled the weak trees, being struck by strong wind from two directions might have increased the uprooting risk for healthy trees. The data in this study describe the RSPs of the trees that had been shaken by strong wind mainly from two directions.

Soil physical properties

Soil solid phase, dry bulk density, and penetration resistances tended to be higher in the second horizons and the deepest horizons (Table 3, Fig. 2a). The RSP of C2, the sample tree closest to soil profile 2 with the lowest penetration resistance, was thicker than those of the other trees (Fig. 2b). The proportions of liquid phase, that is, volumetric soil water contents measured using the soil core samples, were 23.8 ± 8.2%, 21.8 ± 8.5%, and 21.9 ± 10.6% for the uppermost horizon, the subsurface horizon, and the deepest horizon, respectively. These values were similar to those measured using a soil moisture monitor on the day

Table 3 Soil physical properties recorded at the study site (mean ± SD, $n = 6$ soil profiles) on 16–18 January 2019

Soil physical properties/ soil sampling depth	Proportions of the three phases			Bulk density	Penetration resistance	Yamanaka soil hardness index
	Solid	Liquid	Gas			
	(%)	(%)	(%)	(g m^{-3})	(kg cm^{-2})	(mm)
0–10 cm (uppermost)	39.8 ± 9.6	23.8 ± 8.2	36.5 ± 7.9	1.0 ± 0.3	2.56 ± 1.33 (0.25 MPa)	12.37 ± 3.59
35–45 cm (second)	54.0 ± 4.6	21.8 ± 8.5	24.2 ± 12.7	1.4 ± 0.1	7.10 ± 2.26 (0.70 MPa)	19.27 ± 3.03
50–80 cm (deepest)	55.9 ± 4.5	21.9 ± 10.6	22.2 ± 8.5	1.5 ± 0.1	6.02 ± 1.18 (0.59 MPa)	19.15 ± 1.17

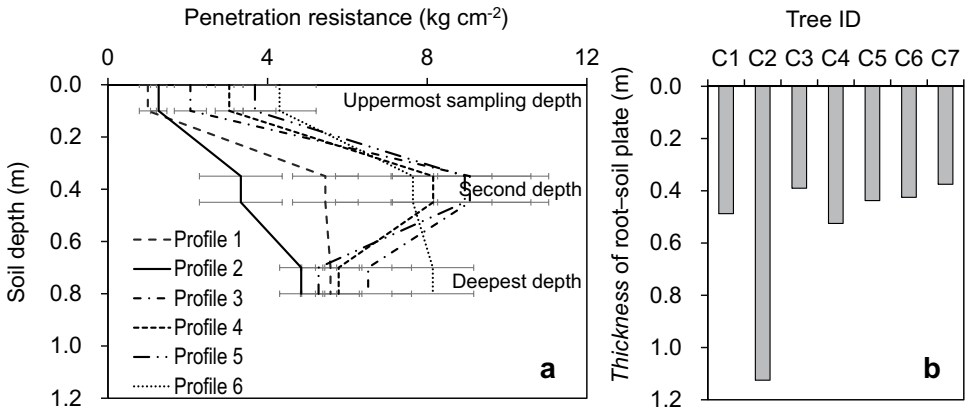

Fig. 2 Profiles of **a** penetration resistance of soil at the study site and **b** thickness of a root–soil plate. Soil profile 2 was collected near C2

of the typhoon (20.2 ± 0.9%, mean ± SD; Takanashi et al., unpublished data). Thus, we used fresh weight of $RSP_{uprooted}$, $Soil_{uprooted}$, and $Root_{uprooted}$ directly measured on the day of RSP dismantling as the fresh weights on the day Typhoon Jebi struck the forest.

Mass and volume of the root–soil plate and aboveground biomass of *Cryptomeria japonica*

The RSP masses of the seven fallen *C. japonica* trees ranged from 251 to 3070 kg, in accord with fluctuation in the DBH, which ranged from 16 to 44 cm (Table 2). Total root biomasses accounted for 5–15% (29–192 kg) with a mean value of 8% of mass of the plate, whereas soil mass made up 85–95% (221–2880 kg) with a mean value of 92% (Table 2, Fig. 3a). Sample tree C1 with DBH of 31 cm, a rotted tree, had a relatively low total root biomass (39 kg) and a lower RSP mass (675 kg). The ratio of soil mass to total root biomass in the RSPs was 13 ± 5 (mean ± SD) (Fig. 3a). The ratio of soil mass to tree biomass was 2.8 ± 1.1 (mean ± SD) (Fig. 3c).

The seven RSPs were in the form of ellipses with radii in the direction of the wind (R_{upper}) and in the direction parallel to the ground ($R_{horizontal}$). Ellipticity, defined as $R_{upper}/R_{horizontal}$ in this study, varied from 0.72 to 1.22 (0.99 ± 0.21, mean ± SD, Table S1 of Supplementary materials). The coefficient of variation of thickness for each RSP ranged from 0.11 to 0.30 (Table S1 of Supplementary materials). The bottoms of the plates reached the second soil horizon, which had higher dry bulk density and penetration resistance than the uppermost horizon (Fig. 2). The hinge ratio varied from 0.23 to 0.57 (0.31 ± 0.12, mean ± SD, Table S1 of Supplementary materials). As DBH increased, $V_{uprooted}$ varied from 0.38 to 3.03 m^3 (Table 2). $V_{uprooted}$ had a significant linear relationship with $RSP_{uprooted}$ (Fig. S4a of Supplementary materials). When C2 (the largest RSP) was excluded, the relationship remained significant (Fig. S4b of Supplementary materials). The gravimetric IT ratio was 96.7 ± 3.2% (mean ± SD) for the seven *C. japonica*. This

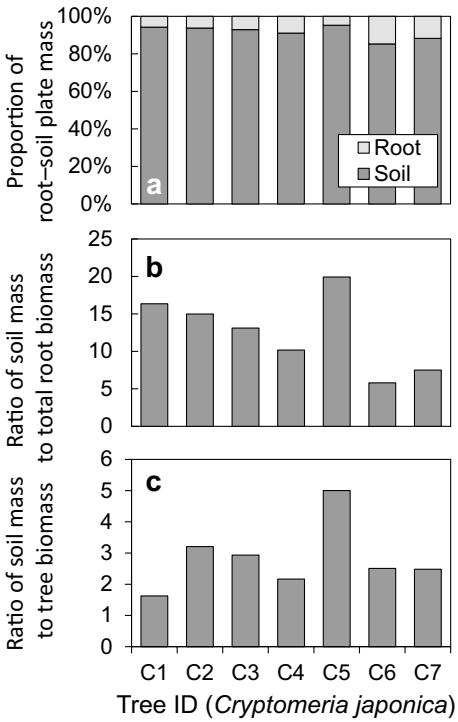

Fig. 3 Contribution of the soil mass or total root biomass to the root–soil plate mass (**a**), the ratio of the soil mass to total root biomass (**b**), and the ratio of the soil mass to the tree biomass

value did not include roots from the tipped-up side that had been torn off by uprooting, since it is difficult to identify which tree roots left in the ground belong to.

Relationships of root–soil plate mass and volume to aboveground allometric indices for *Cryptomeria japonica*

The mean root-to-shoot ratio was 0.26, while the mean ratio of RSP mass to aboveground biomass was 3.9 in the seven sample trees (Fig. 4). The rotted tree, C1, had a much lower ratio of RSP mass to aboveground biomass (1.9) than the

other sample trees. Significant power and linear regression equations were obtained between RSP properties (mass and volume) and the aboveground allometric indices (Table 4, Fig. S5, Fig. S6 of Supplementary materials) as for the seven *C. japonica*. Only stem taper index was negatively proportional to the RSP properties. The power regression was better fit to the data than the linear regression for $RSP_{uprooted}$ and $Soil_{uprooted}$. The relationships of $RSP_{uprooted}$ and $Soil_{uprooted}$ to aboveground properties were stronger than those of $Root_{uprooted}$ and $V_{uprooted}$, regardless of whether mass was determined on a fresh or dried basis. The power multipliers of both $RSP_{uprooted}$ and $Soil_{uprooted}$ were larger than that of $Root_{uprooted}$. Although $RSP_{uprooted}$, $Soil_{uprooted}$, and $V_{uprooted}$ had significant relationships with all of the indices, $Root_{uprooted}$ did not show significant relationships with all of the indices. The trend was more obvious when trees C1 (the rotted tree) and C2 (the tree with the largest RSP by far) were excluded from the analysis. When C1 and C2 were excluded, the power regressions for the relationships between RSP properties and stem biomass or aboveground biomass were not converged.

Radius and thickness of root–soil plate across tree species

Linear regression equations for the relationship between DBH and $2R_{horizontal}$ ($R^2 = 0.82$, $P < 0.001$) and between DBH and thickness ($R^2 = 0.47$, $P < 0.01$) were determined for 13 *C. japonica* (Fig. 5). Because neighboring trees fell onto many of the RSPs in our study site, few of our RSP samples retained their original shape. Therefore, the number of RSP samples was not equal among tree species. To test the second hypothesis, we investigated whether the values of the other tree species fell within the 95% confidence interval (CI) of the regression residuals for *C. japonica*. For $2R_{horizontal}$, several samples were outside the 95% CI. However, the tendency to increase of $2R_{horizontal}$ with DBH was similar for all species, and no species-related bias was detected. For *thickness*, two deep-rooted trees (*C. japonica* and *Quercus acutissima*) were toward the upper edge of the interval, whereas two intermediate-rooted trees (*Q. myrsinifolia*) were toward the lower edge of the interval.

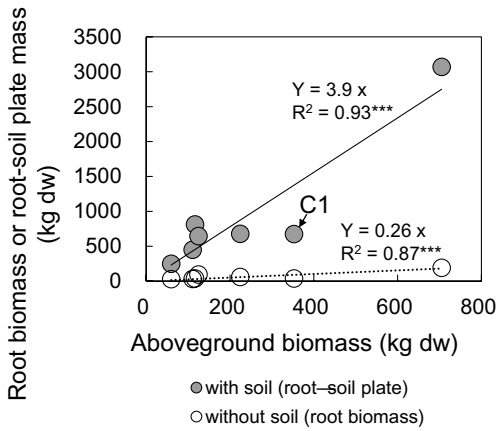

Fig. 4 Linear regression analysis of the relationship between aboveground biomass and total root biomass or root–soil plate mass. Both lines shown indicate a significant relationship. Broken line indicates root-to-shoot ratio, and solid line indicates ratio of root–soil plate mass to aboveground biomass

Discussion

The soil mass held in a root–soil plate of *Cryptomeria japonica*

This is the first study to show quantitatively that roots hold soil with a mass dramatically heavier than the tree biomass. The roots of the *C. japonica* trees held soil weighing up to 13 times their own mass (Fig. 3b). Separate measurement of the soil and roots in RSPs indicated that the soil mass held by a tree's roots was 2.8 times larger than tree biomass (Fig. 3c). The root-to-shoot ratio, indicating biomass allocation, was 0.26 (Fig. 4), which is the same as the average value for temperate forest reported by Cairns et al. (1997) and the average for *C. japonica* calculated using data presented by Fukuda et al. (2003). On the other hand, the ratio of RSP mass to aboveground biomass was 3.9 (Fig. 4), which was much higher than the root-to-shoot ratio (0.26). The soil accounted for 92% of the RSP mass (Fig. 3a) and 72% of the whole-tree mass, including the RSP, the sum of tree biomass and soil mass. In line with our first hypothesis, the soil perhaps compensates for the weight imbalance between above- and belowground, adding additional mass.

Achim and Nicoll (2009) estimated RSP mass from RSP volume using RSP shape parameters, such as radius. Ray and Nicoll (1998) also calculated RSP mass by multiplying volume and soil bulk density, because RSP masses were too large and heavy to weigh directly. This study confirmed that $V_{uprooted}$ was linearly proportional to $RSP_{uprooted}$ (Fig. S4 of Supplementary materials). Measurement of radius and thickness of RSP can help to estimate the uprooted RSP mass via its volume.

Downward development of the root–soil plates

The lower edge of the RSPs of the seven *C. japonica* reached nearly to the second soil sampling depth (Fig. 2); this horizon had higher solid phase, dry bulk density, and penetration resistance than soil at the uppermost sampling depth (Table 3). The ability of plant roots to penetrate soils is restricted as soil strength increases (Hamza and

Table 4 Regression coefficients and coefficient of determination of power and linear regression analyses of root–soil plate (RSP) mass or volume to aboveground allometric indices for *Cryptomeria japonica* trees

x	DBH (cm)			Stem biomass (kg)			Aboveground biomass (kg)			H×DBH^2 (m^3)			Stem taper index		
y Power regression ($y=ax^b$)															
Mass or volume	a	b	R^2	a	b	R^2	a	b	R^2	a	b	R^2	a	b	R^2
All samples (n=7)															
$RSP_{uprooted}$ (kg fw)[a,b]	0.19	2.5	0.92***	1.5	1.2	0.88**	1.52	1.1	0.87**	534	1.1	0.88**	6.43×10^{10}	−4.4	0.99***
$RSP_{uprooted}$ (kg dw)[a]	0.13	2.6	0.93***	1.1	1.2	0.89**	1.18	1.1	0.89**	421	1.1	0.89**	3.13×10^{10}	−4.3	0.99***
$Soil_{uprooted}$ (kg fw)[a,b]	0.12	2.6	0.93***	1.1	1.2	0.88**	0.98	1.2	0.88**	445	1.1	0.89**	4.83×10^{10}	−4.3	0.99***
$Soil_{uprooted}$ (kg dw)[a]	0.10	2.6	0.93***	0.94	1.2	0.89**	0.83	1.2	0.89**	383	1.1	0.90**	2.90×10^{10}	−4.3	0.99***
$Root_{uprooted}$ (kg fw)[a,b]	0.16	2.0	0.73*	–	–	NC	–	–	NC	88	0.8	0.69*	1.42×10^{14}	−6.9	0.83**
$Root_{uprooted}$ (kg dw)[a]	0.06	2.0	0.74*	–	–	NC	0.69	0.78	0.68*	38	0.8	0.69*	3.15×10^{11}	−5.6	0.82**
$V_{uprooted}$ (m^3) [a]	0.0007	2.2	0.87**	0.005	1.0	0.82**	0.003	0.89	0.80**	0.77	0.93	0.82**	2.13×10^{8}	−4.7	0.97***
Samples excluding C1 and C2 (n=5)															
$RSP_{uprooted}$ (kg dw)[a]	0.48	2.2	0.96**	–	–	NC	–	–	NC	570	1.0	0.89*	–	–	NC
$Soil_{uprooted}$ (kg dw)[a]	0.24	2.4	0.93**	–	–	NC	–	–	NC	518	1.0	0.83*	–	–	NC
$Root_{uprooted}$ (kg dw)[a]	–	–	NS	–	–	NS	–	–	NS	–	–	NS	–	–	NS
$V_{uprooted}$ (m^3)[a]	–	–	NC	–	–	NC	–	–	NC	–	–	NS	–	–	NS
y Linear regression ($y=cx+d$)															
Mass or volume	c	d	R^2	c	d	R^2	c	d	R^2	c	d	R^2	c	d	R^2
All samples (n=7)															
$RSP_{uprooted}$ (kg fw)[a,b]	78.6	−1191	0.83**	4.95	−48.8	0.86**	3.24	23.6	0.85**	574	−12.2	0.85**	−51.1	4496	0.76*
$RSP_{uprooted}$ (kg dw)[a]	64.9	−1002	0.85**	4.08	−59.0	0.87**	2.68	−0.98	0.87**	473	−27.9	0.86**	−42.1	3691	0.77**
$Soil_{uprooted}$ (kg fw)[a,b]	70.3	−1091	0.84**	4.42	−69.5	0.86**	2.89	−4.68	0.86**	513	−37.3	0.86**	−46.0	4016	0.78**
$Soil_{uprooted}$ (kg dw)[a]	61.3	−958	0.85**	3.86	−67.3	0.87**	2.53	−11.7	0.87**	447	−38.4	0.87**	−39.9	3482	0.78**
$Root_{uprooted}$ (kg fw)[a,b]	8.2	−98.0	0.67*	0.52	20.9	0.70*	0.34	28.5	0.70*	60.1	25.4	0.69*	–	–	NS
$Root_{uprooted}$ (kg dw)[a]	3.6	−43.9	0.69*	0.23	8.30	0.71*	0.15	11.6	0.71*	26.2	10.4	0.69*	–	–	NS
$V_{uprooted}$ (m^3)[a]	0.087	−1.17	0.80**	0.006	−0.08	0.86**	0.004	0.022	0.83**	0.72	−0.029	0.84**	−0.07	6.01	0.88*
Samples excluding C1 and C2 (n=5)															
$RSP_{uprooted}$ (kg dw)[a]	47.5	−588	0.97**	4.38	−26.8	0.87*	–	–	NS	600	−27.0	0.89*	−16.2	1654	0.93**
$Soil_{uprooted}$ (kg dw)[a]	43.9	−550	0.94**	4.00	−23.2	0.80*	–	–	NS	545	−23.8	0.83*	−15.6	1570	0.97**
$Root_{uprooted}$ (kg dw)[a]	–	–	NS	–	–	NS	–	–	NS	–	–	NS	–	–	NS
$V_{uprooted}$ (m^3)[a]	–	–	NS	–	–	NS	–	–	NS	–	–	NS	–	–	NS

[a]Subscript "uprooted" indicates data for uprooted RSPs, excluding the hinge side (see Fig. 1)

[b]Fresh weights were directly measured, not calculated

*, **, and *** indicate significance at $P<0.05$, 0.01, and 0.001, respectively; NS indicates not significant at $P\geq0.05$; NC indicates not converged

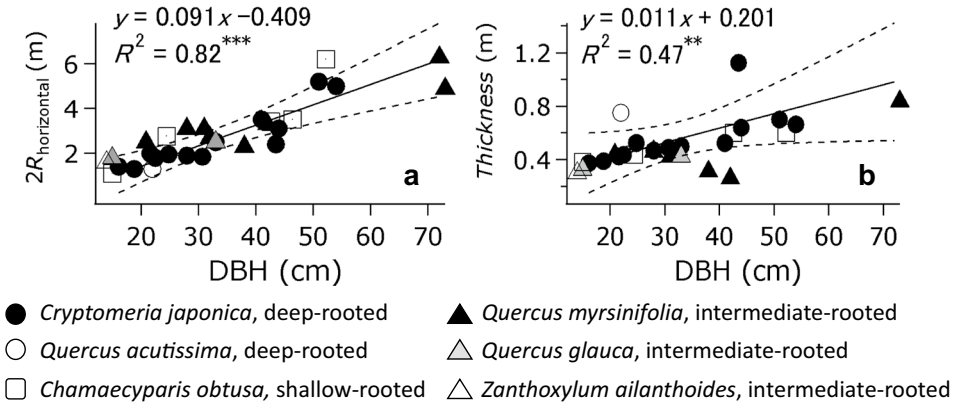

Fig. 5 Relationships of DBH to $2R_{horizontal}$ and thickness of root–soil plates for different tree species. Solid lines show the linear relationship for the 13 *Cryptomeria japonica*, and the broken lines show the 95% confidence interval of the regression residuals

Anderson 2005). McKenzie et al. (2004) reported that dry bulk density greater than about 1.6 g m^{-3} restricted root elongation. Similarly, Simmons and Pope (1987) reported that root elongation was impeded at dry bulk density greater than 1.40 g m^{-3}. The dry bulk density of the soils around the bottoms of the RSPs (i.e., second soil sampling depth) was close to these values (1.4–1.5 g m^{-3}, Table 3). Although the critical dry bulk density that restricts root growth depends on soil type (Hunt and Gilkes 1992) and axial root growth pressure depends on plant species (Taylor and Willatt 1983), root downward elongation may have been restricted in this forest. In fact, all sampled RSPs were flat regardless of tree species, and roots easily distinguishable as taproots were not found during examination of *C. japonica* RSPs.

In line with our second hypothesis, RSP thickness was roughly the same, regardless of species-specific root architecture, when standardized by tree size (Fig. 5b). RSP thickness for almost all tree species, including shallow-rooted trees, fell within the 95% CI of the regression residuals of *C. japonica*, a deep-rooted tree. The increasing thickness with increasing DBH implies that root elongation had not stopped entirely, and the downward development of RSPs continued to progress. Downward development may have been as slow in deep-rooted trees as in shallow-rooted trees, owing to the high penetration resistance of the soil, which would have restricted expression of species-specific root architecture. Two deep-rooted trees (*C. japonica* and *Q. acutissima)* were toward the upper edge of the 95% CI, whereas two intermediate-rooted trees (*Q. myrsinifolia*) were toward the lower edge of the 95% CI. If these two deep-rooted trees were growing in soft spots in the hard soil, their RSPs could have become thicker than the others. Similarly, when shallow- or intermediate-rooted trees were growing in especially hard spots in the soil, their RSPs may have become thinner than the others.

The ratio of soil mass to total root biomass (13), may reflect RSP formation efficiency. If the soil has high dry bulk density, a relatively small quantity of roots can hold a high soil mass. Instead, high penetration resistance may restrict formation of taproots, the most effective root component for anchorage (Yang et al. 2017). Therefore, this ratio may vary depending on the combination of root system architecture and soil properties.

Radius of root–soil plate across tree species

The RSPs of most species fell within the 95% CI of the regression residuals of the linear relationship between DBH and $2R_{horizontal}$ for *C. japonica* (Fig. 5a). However, several trees did not. Regarding our second hypothesis, we conclude that RSPs of trees growing in hard soil are likely to have a similar if not identical form.

The ratio of RSP radius to DBH represents part of the area into which the root system penetrates. According to Danjon et al. (2005), the main sinker root volume (70%) is located within a radius of just over twice the tree's DBH. The area forms a solid cage to hold soil mass within a zone of rapidly tapering roots, which rarely breaks during uprooting. In the case of *Pinus pinaster* which forms deep root systems, the RSP radius equals 2.2 × DBH (Danjon et al. 2005). In this study, the ratio of $R_{horizontal}$ to DBH was 4.1, or half of the regression coefficient (8.1) in the regression equation between DBH and $R_{horizontal}$. Examining the ratio of RSP radius to stem radius (half the DBH) was proposed by Mattheck et al. (1993), who indicated the ratio produced a curve that decreased with increasing stem radius for both *Picea abies* and other species having flat RSPs. The distribution of the ratios in this study completely overlapped with the variance of the curve for this relationship for shallow-rooted trees produced by Mattheck et al. (1993) (data not shown). Deep-rooted tree species grow roots in the horizontal direction when their downward elongation is limited by soil environments (Hirano et al. 2018). Therefore, not only shallow-rooted trees, but deep-rooted trees with root systems that develop horizontally instead of downward would tend to have a larger RSP radius. This is in line with the observation

of Ray and Nicoll (1998), that the RSP radius of *P. sitchensis* increased when limited by the soil moisture environment.

The gravimetric IT ratio was as high as 97%, meaning that most roots were within the RSPs. Because this value did not include roots on the tipped-up side that were torn off by uprooting, we calculated the volumetric IT ratio for *C. japonica* trees in the same study site that were not felled by the storm. The root systems of the three *C. japonica* (roots A, B, and C) were carefully excavated and were used for a study focusing on reconstruction of root system architecture using root point coordinates and diameters (Ohashi et al. 2019). Although fine roots < 2 mm in diameter were removed, most roots larger than 2–5 mm in diameter remained. The root point coordinates were connected by virtual cylinders, and the IT ratio was calculated on a volumetric basis. Determination of the RSP radius of Roots A–C was performed using DBH, as described above. The direction of collapse due to wind damage is unknown in advance, so we determined the mean of $R_{\mathrm{horizontal}}$ and R_{upper} for C1–C7, and divided this mean value by DBH. The RSP radius was 3.75 times the DBH, on average, for the seven *C. japonica*. Using this value, the volumes of Roots A–C were divided into inside and outside roots. The volumetric IT ratios were 98.0%, 97.8%, and 98.7% for roots A, B, and C, respectively (Fig. S7 of the Supplementary materials). The lower boundary of the RSP was considered for the IT ratios of C1–C7, but not for those of Roots A–C. Nevertheless, the IT ratios of C1–C7 were very similar to those of Roots A–C. Therefore, we conclude that the biomass of outside roots accounts for only a few percent of the total root biomass, and the RSP area included most of the roots beneath each *C. japonica* tree in our study site.

Relationships of root–soil plate mass and aboveground allometric indices of *Cryptomeria japonica*

Due to the difficulty of estimating root anchorage nondestructively, it is commonly estimated by aboveground tree size, such as $H \times \mathrm{DBH}^2$ (Cucchi et al. 2004; Hale et al. 2012; Kamimura et al. 2012; Lundström et al. 2007a, b; Nicoll et al. 2006; Peltola et al. 2000). This study is the first to validate that uprooted RSP properties is directly proportional to aboveground allometric indices (Table 4, Fig. S5, 6 of Supplementary materials). The power multipliers of both $\mathrm{RSP}_{\mathrm{uprooted}}$ and $\mathrm{Soil}_{\mathrm{uprooted}}$ were larger than that of $\mathrm{Root}_{\mathrm{uprooted}}$, indicating that RSP development rate was higher than the root development rate. Longer roots formed as trees grow may efficiently enclose a larger amount of soil. This is in line with the suggestion by Ennos (1993) that RSP becomes more efficient at large tree size, because the energetic cost of RSP construction becomes relatively cheaper with plant growth. Ennos (1993) pointed out that anchorage provided by the RSP mass increases with the fourth power of linear dimensions rather than with their cube; however, our power multipliers did not reach four. Even as roots enclose larger areas of soil, promoting tree stability, the potential turning moment created by the concurrently heightening stem and crown area may threaten it. To understand tree stability, we need to evaluate the two opposite contributions of enclosing soil with roots.

The RSP properties were negatively proportional to the stem taper index (*H*/DBH ratio), an important index of tree stability with respect to stem failure (Cremer et al. 1982; Petty and Swain 1985). This result suggests that a tree with higher stem taper has a lighter RSP because the amount of soil held within the plate is reduced. A lighter RSP could be one of the factors that impairs the stability of trees with a highly tapered stem.

When data for trees C1 and C2 were excluded, the relationships of $\mathrm{RSP}_{\mathrm{uprooted}}$ and $\mathrm{Soil}_{\mathrm{uprooted}}$ to many indices remained significant, whereas the relationships of $\mathrm{Root}_{\mathrm{uprooted}}$ and V_{uprooted} to all indices became insignificant ($P > 0.05$). Therefore, the relationship of soil mass to aboveground indices appears to be more robust than those of root biomass or RSP volume.

Limitations of this study

Removal of storm debris to restore safety was the highest priority at our study site, where the forest was severely damaged by the typhoon. Because cleanup of the forest site was urgent, we could not measure aboveground biomass. Stem biomass and aboveground biomass were not robust indices of RSP mass (Table 4), because the relationships were not significant when C1 and C2 were excluded from the regression analysis. In future studies, we should measure biomass directly instead of estimating it.

Simplification of the spatial variation of soil structure may impact prediction of tree uprooting, RSP shape, and the critical bending moment (Yang et al. 2020). Further, we were unable to consider the root architecture of individual sample trees. The most effective root structures for forming a "cage" enclosing soil are the "zone of rapid taper" defined by Danjon et al. (1999a, b) and the sinker roots (Danjon et al. 2005). The zone of rapid taper is one of the predominant factors in critical turning moment (Yang et al. 2018). Because we used a chainsaw to divide the RSP piece by piece to carefully collect even soil that was bound very tightly to the roots, it was impossible to collect data on the size or shape of the root cage. Thus, the associations between root architecture and RSP size as trees grow remains to be clarified.

Conclusions

This study is the first to show quantitatively that roots hold soil that is dramatically heavier than tree biomass. Because for trees with a plate-like root system soil mass is more important than soil shear strength (Mattheck et al. 2015), we dismantled flat RSPs formed in hard soil to evaluate soil mass. The roots enclosed soil 2.8 times heavier than tree biomass. Thus, the soil held by a tree's roots would alter the belowground to aboveground weight balance ratio from 0.26 (total root biomass only) to 3.9 (with soil), providing additional anchorage. We also verified that aboveground allometric indices are good indicators of RSP mass and volume. In regression analyses with aboveground allometric indices, the power multipliers of RSPs were larger than those of roots, suggesting that trees expand RSPs at an accelerated rate as they grow. Multiple species with different types of root architecture showed similar radius and thickness of RSP in the hard forest soil, likely because the soil hardness prevented them from exhibiting their characteristic root shapes. Further research is needed to clarify the associations between RSP development and (1) tree growth, and (2) development of root structures that form soil "cages", such as a zone of rapid taper. Gaining a better understanding of these associations will help to develop and manage forests with a higher tolerance against wind damage.

Author contributions statement Conceptualization: TT, YH. Methodology: TT, YH, YI. Software: HI, CT. Formal analysis and investigation: all authors. Writing: TT, HI, YI.

Acknowledgements We greatly appreciate S. Narayama, T. Chikaguchi, M. Tanaka, K. Takahashi, H. Kobayashi, S. Takanashi, Y. Yamamoto, Y. Shimada, J. An, and the other Forestry and Forest Products Research Institute (FFPRI) members, K. Goto, Y. Okamoto (University of Hyogo), and Y. Matsuda (son of T. Tanikawa) for associating our field study. We also thank K. Nanko (FFPRI), A. Sumida (Hokkaido University), and N. Hijii (Nagoya University), Y. Matsuda (Mie University) for discussing tree stability or forest ecology with us, R. Doi, G. Yoshida, and R. Nishimura (Nagoya University) for help measuring soil physical properties.

Funding This study was supported by a KAKENHI Grant (No. JP20H03040, JP20H03028) from the Japan Society for the Promotion of Science, and by the Program to supporting research activities of female researchers funded by the MEXT Special Coordination Fund for Promoting Science and Technology.

Compliance with ethical standards

Conflict of interest The authors declare that they have no conflicts of interests.

References

Achim A, Nicoll BC (2009) Modelling the anchorage of shallow-rooted trees. Forestry 82:273–284. https://doi.org/10.1093/forestry/cpp004

Cairns MA, Brown S, Helmer EH, Baumgardner GA (1997) Root biomass allocation in the world's upland forests. Oecologia 111:1–11. https://doi.org/10.1007/s004420050201

Clark LJ, Whalley WR, Barraclough PB (2003) How do roots penetrate strong soil? In: Abe JJ (ed) Roots: the dynamic interface between plants and the earth. Springer, Dordrecht, pp 93–104

Coutts MP (1983) Root architecture and tree stability. Plant Soil 71:171–188. https://doi.org/10.1007/BF02182653

Coutts MP (1986) Components of tree stability in sitka spruce on peaty gley soil. Forestry 59:173–197. https://doi.org/10.1093/forestry/59.2.173

Cremer KW, Borough CJ, McKinnell FH, Carter PR (1982) Effects of stocking and thinning on wind damage in plantations. N Z J For Sci 12:224–268

Crook MJ, Ennos AR (1998) The increase in anchorage with tree size of the tropical tap rooted tree *Mallotus wrayi*, King (Euphorbiaceae). Ann Bot 82:291–296. https://doi.org/10.1006/anbo.1998.0678

Crook MJ, Ennos AR, Banks JR (1997) The function of buttress roots: a comparative study of the anchorage systems of buttressed (Aglaia and *Nephelium ramboutan* species) and non-buttressed (*Mallotus wrayi*) tropical trees. J Exp Bot 48:1703–1716. https://doi.org/10.1093/jxb/48.9.1703

Cucchi V, Meredieu C, Stokes A, Berthier S, Bert D, Najar M, Denis A, Lastennet R (2004) Root anchorage of inner and edge trees in stands of Maritime pine (*Pinus pinasterAit.*) growing in different podzolic soil conditions. Trees 18:460–466. https://doi.org/10.1007/s00468-004-0330-2

Danjon F, Bert D, Godin C, Trichet P (1999a) Structural root architecture of 5-year-old *Pinus pinaster* measured by 3D digitising and analysed with AMAPmod. Plant Soil 217:49–63. https://doi.org/10.1007/978-94-017-3469-1_6

Danjon F, Sinoquet H, Godin C, Colin F, Drexhage M (1999b) Characterisation of structural tree root architecture using 3D digitising and AMAPmod software. Plant Soil 211:241–258. https://doi.org/10.1023/A:1004680824612

Danjon F, Fourcaud T, Bert D (2005) Root architecture and wind-firmness of mature *Pinus pinaster*. New Phytol 168:387–400. https://doi.org/10.1111/j.1469-8137.2005.01497.x

Dorval AD, Meredieu C, Danjon F (2016) Anchorage failure of young trees in sandy soils is prevented by a rigid central part of the root system with various designs. Ann Bot 118:747–762. https://doi.org/10.1093/aob/mcw098

Dupuy L, Fourcaud T, Stokes A (2005a) A numerical investigation into the influence of soil type and root architecture on tree anchorage. Plant Soil 278:119–134. https://doi.org/10.1007/s11104-005-7577-2

Dupuy L, Fourcaud T, Stokes A (2005b) A numerical investigation into factors affecting the anchorage of roots in tension. Eur J Soil Sci 56:319–327. https://doi.org/10.1111/j.1365-2389.2004.00666.x

Dupuy LX, Fourcaud T, Lac P, Stokes A (2007) A generic 3D finite element model of tree anchorage integrating soil mechanics and real root system architecture. Am J Bot 94:1506–1514. https://doi.org/10.3732/ajb.94.9.1506

Ennos AR (1993) The scaling of root anchorage. J Theor Biol 161:61–75. https://doi.org/10.1006/jtbi.1993.1040

Forest Agency of Japan (2012) Annual Report on Trends in Forests and Forestry 2011. Tokyo (in Japanese)

Forestry and Forest Product Research Institute (2010) Stem volume calculation program. Forestry and Forest Product Research Institute

web site. https://www.ffpri.affrc.go.jp/database/stemvolume/index.html. Accessed 12 Jul 2020 **(in Japanese)**

Fourcaud T, Ji JN, Zhang ZQ, Stokes A (2008) Understanding the impact of root morphology on overturning mechanisms: a modelling approach. Ann Bot 101:1267–1280. https://doi.org/10.1093/aob/mcm245

Fukuda M, Iehara T, Matsumoto M (2003) Carbon stock estimates for sugi and hinoki forests in Japan. For Ecol Manag 184:1–16. https://doi.org/10.1016/S0378-1127(03)00146-4

Ghani MA, Stokes A, Fourcaud T (2009) The effect of root architecture and root loss through trenching on the anchorage of tropical urban trees (*Eugenia grandis* Wight). Trees 23:97–209. https://doi.org/10.1007/s00468-008-0269-9

Hale SE, Gardiner BA, Wellpott A, Nicoll BC, Achim A (2012) Wind loading of trees: influence of tree size and competition. Eur J For Res 131:203–217. https://doi.org/10.1007/s10342-010-0448-2

Hamza MA, Anderson WK (2005) Soil compaction in cropping systems: a review of the nature, causes and possible solutions. Soil Tillage Res 82:121–145. https://doi.org/10.1016/j.still.2004.08.009

Hirano Y, Todo C, Yamase K, Tanikawa T, Dannoura M, Ohashi M, Doi R, Wada R, Ikeno H (2018) Quantification of the contrasting root systems of *Pinus thunbergii* in soils with different groundwater levels in a coastal forest in Japan. Plant Soil 426:327–337. https://doi.org/10.1007/s11104-018-3630-9

Hosoda K, Mitsuda Y, Iehara T (2010) Differences between the present stem volume tables and the values of the volume equations, and their correction. Jpn J For Plann 44:23–39. https://doi.org/10.2059/jjfp.44.2_23 (**in Japanese with English abstract**)

Hunt N, Gilkes RJ (1992) Farm monitoring handbook. The University of Western Australia, Nedlands, WA (indirectly cited)

Inagaki Y, Nakanishi A, Tange T (2020) A simple method for leaf and branch biomass estimation in Japanese cedar plantations. Trees 34:349–356. https://doi.org/10.1007/s00468-019-01920-8

Jahn R, Blume HP, Asio VB, Spaargaren O, Schad P (2006) Guidelines for soil description. FAO, Rome

Kamimura K, Kitagawa K, Saito S, Mizunaga H (2012) Root anchorage of hinoki (*Chamaecyparis obtusa* (Sieb. Et Zucc.) Endl.) under the combined loading of wind and rapidly supplied water on soil: analyses based on tree-pulling experiments. Eur J For Res 131:219–227. https://doi.org/10.1007/s10342-011-0508-2

Karizumi N (2010) The latest illustrations of tree roots. Seibundo Shinkosha Poblishing Co Ltd, Tokyo

Khuder H, Stokes A, Danjon F, Gouskou K, Lagane F (2007) Is it possible to manipulate root anchorage in young trees? Plant Soil 294:87–102. https://doi.org/10.1007/s11104-007-9232-6

Klepper B (1991) Root-shoot relationships. In: Waisel Y, Eshel A, Kafkafi U (eds) Plant roots: the hidden half. Marcel Dekker, New York, pp 265–286

Köstler JN, Brückner E, Bibelriether H (1968) Die Wurzeln der Waldbäume. Verlag Paul Parey, Hamburg, Berlin, Germany (indirectly cited)

Kyoto Local Meteorological Office (2018) Information about the storm caused by Typhoon No. 21 on September 4, 2018 (Preliminary weather report for Kyoto Prefecture). https://www.jma-net.go.jp/kyoto/data/kishousokuhou2018T21.pdf. Accessed 20 Feb 2020 **(in Japanese)**

Lundström T, Jonas T, Stöckli V, Ammann W (2007a) Anchorage of mature conifers: resistive turning moment, RSP geometry and root growth orientation. Tree Physiol 27:1217–1227. https://doi.org/10.1093/treephys/27.9.1217

Lundström T, Jonsson MJ, Kalberer M (2007b) The root—soil system of Norway spruce subjected to turning moment: resistance as a function of rotation. Plant Soil 300:35–49. https://doi.org/10.1007/s11104-007-9386-2

Mattheck C, Bethge K, Erb D (1993) Failure criteria for trees. Arboric J 17:201–209. https://doi.org/10.1080/03071375.1993.9746963

Mattheck C, Bethge K, Weber K (2015) The body language of trees. In: Encyclopedia of visual tree assessment, 1st edn. Karlsruhe Institute of Technology, Karlsruhe

McKenzie N, Jacquier D, Isbell R, Brown K (2004) Australian soils and landscapes: an illustrated compendium. CSIRO Publishing, Victoria

Ministry of Agriculture, Forestry and Fisheries (2019) Report of Typhoon No. 21 (2018). Ministry of Agriculture, Forestry and Fisheries web site. https://www.maff.go.jp/j/saigai/typhoon/20180904.html. Accessed 12 July 2020 **(in Japanese)**

Mokany K, Raison RJ, Prokushkin AS (2006) Critical analysis of root: Shoot ratios in terrestrial biomes. Glob Chang Biol 12:84–96. https://doi.org/10.1111/j.1365-2486.2005.001043.x

Nanko K, Suzuki S, Noguchi H, Ishida Y, Levia DF, Ogura A, Hagino H, Matsumoto H, Takimoto H, Sakamoto T (2019) Mechanical properties of Japanese black pine (*Pinus thunbergii* Parl.) planted on coastal sand dunes: resistance to uprooting and stem breakage by tsunamis. Wood Sci Technol 53:469–489. https://doi.org/10.1007/s00226-019-01078-z

Nicoll BC, Gardiner BA, Rayner B, Peace AJ (2006) Anchorage of coniferous trees in relation to species, soil type, and rooting depth. Can J For Res 36:1871–1883. https://doi.org/10.1139/X06-072

Ohashi M, Ikeno H, Sekihara K, Tanikawa T, Dannoura M, Yamase K, Todo C, Tomita T, Hirano Y (2019) Reconstruction of root systems in *Cryptomeria japonica* using root point coordinates and diameters. Planta 249:445–455. https://doi.org/10.1007/s00425-018-3011-x

Peltola H, Kellomäki S, Hassinen A, Granander M (2000) Mechanical stability of Scots pine, Norway spruce and birch: an analysis of tree-pulling experiments in Finland. For Ecol Manage 135:143–153. https://doi.org/10.1016/S0378-1127(00)00306-6

Petty JA, Swain C (1985) Factors influencing stem breakage of conifers in high winds. Forestry 58:75–85. https://doi.org/10.1093/forestry/58.1.75

R Core Team (2019) R: A language and environment for statistical computing (Version 3.5.3). R Foundation for Statistical Computing, Vienna, Austria. https://www.R-project.org/

Ray D, Nicoll BC (1998) The effect of soil water-table depth on root-plate development and stability of Sitka spruce. Forestry 71:169–182. https://doi.org/10.1093/forestry/71.2.169

Sagi P, Newson T, Miller C, Mitchell S (2019) Stem and root system response of a Norway spruce tree (*Picea abies* L.) under static loading. For An Int J For Res 92:460–472. https://doi.org/10.1093/forestry/cpz042

Shinozaki K, Yoda K, Hozumi K, Kira T (1964) A quantitative analysis of plant form- the pipe model theory. I. Basic analysis. Jpn J Ecol 14:97–105. https://doi.org/10.18960/seitai.14.3_97

Simmons GL, Pope PE (1987) Influence of soil compaction and vesicular–arbuscular mycorrhizae on root growth of yellow poplar and sweet gum seedlings. Can J For Res 17:970–975. https://doi.org/10.1139/x87-151

Soil Survey Staff (2014) Keys to Soil Taxonomy, 12th ed. USDA-NRCS, US Gov. Print. Office, Washington, DC

Stokes A (1999) Strain distribution during anchorage failure of *Pinus pinaster* Ait. at different ages and tree growth response to wind-induced root movement. Plant Soil 217:17–27. https://doi.org/10.1023/A:1004613126353

Stokes A, Fitter AH, Coutts MP (1995) Responses of young trees to wind and shading: effects on root architecture. J Exp Bot 46:1139–1146. https://doi.org/10.1093/jxb/46.9.1139

Takabatake T, Mäll M, Esteban M, Nakamura R, Kyaw TO, Ishii H, Valdez JJ, Nishida Y, Noya F, Shibayama T (2018) Field survey of 2018 Typhoon Jebi in Japan: lessons for disaster risk management. Geosci 8:412. https://doi.org/10.3390/geosciences8110412

Taylor HM, Willatt ST (1983) Shrinkage of Soybean Roots 1. Agron J 75:818–820. https://doi.org/10.2134/agronj1983.00021962007500050020x

Todo C, Tokoro C, Yamase K, Tanikawa T, Ohashi M, Ikeno H, Dannoura M, Miyatani K, Doi R, Hirano Y (2019) Stability of *Pinus thunbergii* between two contrasting stands at differing distances from the coastline. For Ecol Manage 431:44–53. https://doi.org/10.1016/j.foreco.2018.05.040

Toral M, Bown HE, Mañon A, Alvarez J, Navarro-Cerrillo R (2011) Wind-induced leaning (toppling) in young *Pinus radiata* plantations in Chile. Cienc Investig Agrar 38:405–414. https://doi.org/10.4067/s0718-16202011000300010

Vogt KA, Vogt DJ, Brown S, Tilley JP, Edmonds RL, Silver WL, Siccama TG (1995) Dynamics of forest floor and soil organic matter accumulation in boreal, temperate, and tropical forests. In: Lal R, Kimble J, Levine E, Stewart BA (eds) Soil management and greenhouse effect. CRC Lewis Publishers, Boca Raton, pp 159–178

Yamanaka K, Matsuo K (1962) A study on soil hardness (first report): relationship between soil hardness and water content. J Sci Soil Manure Japan 33–7:343–347 **(in Japanese)**

Yang M, Défossez P, Danjon F, Dupont S, Fourcaud T (2017) Which root architectural elements contribute the best to anchorage of Pinus species? Insights from in silico experiments. Plant Soil 411:275–291. https://doi.org/10.1007/s11104-016-2992-0

Yang M, Défossez P, Danjon F, Fourcaud T (2018) Analyzing key factors of roots and soil contributing to tree anchorage of Pinus species. Trees 32:703–712. https://doi.org/10.1007/s00468-018-1665-4

Yang M, Défossez P, Dupont S (2020) A root-to-foliage tree dynamic model for gusty winds during windstorm conditions. Agric For Meteorol 287:107949. https://doi.org/10.1016/j.agrformet.2020.107949